RESEARCH ARTICLE

Grid Forming Control for Power Converters Based on an Inertial Phase Locked Loop (IPLL)

ANDRES TARRASÓ [1,2], (Member, IEEE), **JOSE IGNACIO CANDELA** [1], (Member, IEEE), **JOAN ROCABERT** [1], (Member, IEEE), **ZORAN MILETIC** [2], (Senior Member, IEEE), **AND ALVARO LUNA** [1], (Member, IEEE)

[1]Renewable Electrical Energy Systems (SEER), Technical University of Catalonia, 08222 Terrassa, Spain
[2]AIT Austrian Institute of Technology GmbH, 1210 Vienna, Austria

Corresponding author: Andres Tarrasó (andres.tarraso@upc.edu)

ABSTRACT Inertia emulation is claimed to play a decisive role in the regulation and management of frequency in modern electrical systems. The support offered by renewable energy power plants and distributed generators is key to diminish the rate of change of frequency (RoCoF), as many synchronous generators are being replaced all around the globe. It is a reality that the implementation of the swing equation in the power converter control has been the core of several proposals on grid-forming controllers to emulate inertia. This kind of controller has been heavily studied and integrated in some demonstrators around the world during the last years, providing dynamic inertia support functionalities. However, the need to modify the synchronization strategy in already deployed power units has been one of the key opposition factors on industry, leading to a severe shortcoming on the integration. In contrast to the traditional swing equation implementation this paper presents a lightweight inertial phase-locked loop (IPLL) able to take the most of inertial features introducing minor changes on classical power converter control and synchronization structures. As shown in this work, the straightforward implementation significantly reduces the technological and computational effort compared to other synchronous emulation proposals. Moreover, it integrates not only dynamic inertial response to the converter, but also all grid-forming capacities to the power conversion unit. This modification on the synchronization structure enables the converter to work in grid-following mode in grid-tied applications, and grid-forming in islanded ones. The integration of the proposed IPLL, the stability analysis and a sample of its performance in HIL and experimental environments will be presented in this paper.

INDEX TERMS Phase-locked loop, power converter, power converter control, renewable energy systems, swing equation.

I. INTRODUCTION

During the last century electrical energy systems have relied on synchronous generators to energize and regulate the electrical networks all around the globe [1]. This dependency on synchronous generation has been vital for the stability of the network, however, the massive installation of wind and solar farms, connected at medium voltage networks, as well as the proliferation of small distributed generators interfaced by power converters in low voltage systems, is

The associate editor coordinating the review of this manuscript and approving it for publication was Reinaldo Tonkoski [ID].

changing the paradigm of energy generation, distribution and consumption [2].

The PV power installed in Europe has substantially grown in Europe during the last decade. In fact, it increased 47% in 2022, adding 41.4 GW new installed capacity in Europe [3]. This trend is expected to grow exponentially, giving rise to a massive integration of PV power in the electrical networks, while other energy sources such as coal, gas or nuclear decrease in the mix, giving rise to a remarkable decrease of synchronous generation in the power system, and hence a serious issue regarding inertia availability in the grid.

Despite the feasibility of integrating renewable energy systems in the existing electrical networks [4], the addition of these distributed generators introduce new challenges for grid operators, especially due to their stochastic generation profiles and the lack of inherent grid support performance. Furthermore, the replacement of traditional generation units for renewable energy sources may be an issue for the stability and the reliable response of power systems during grid contingencies [5]. In this scenario, transmission system operators (TSOs) have increased the requirements and modified grid codes for this newly integrated 'non-synchronous' devices [6].

In the last years, several proposals based on designing control algorithms that resemble the effect of synchronous generators [7] have been presented to address this loss on inertial support. In this regard, virtual synchronous machines, have gathered a lot of attention during the last decade [8]. Some of the approaches have used direct voltage control strategies focused on emulating the electromotive force of the generator. Among them, the synchronverter [9] is maybe the most popular one. In fact some improvements on this strategy have been also published, such as the one in [10], where, a self-synchronized system was presented. Likewise, an additional virtual impedance was set to regulate harmonics as a contribution in [11]. However, and despite the fact that those grid-forming controls were feasible and operational, the industry still relies on the robust current control to regulate the current during grid perturbations [12].

Current controlled devices have been always easier to regulate, compared to voltage controlled ones, by its inherent limitation of the current, which lead to a massive integration in industry. Due to this, some new approaches of the grid-forming control arouse based on the premise that a current controller should be the basis for new developments [13]. The most iconic structure for this approach is the synchronous power control (SPC) [14], which generates a current reference by using a virtual admittance (VA) [15]. This idea of synchronous generation changed the synchronization structure from the classical phase-locked loop (PLL) voltage synchronization to the swing equation power synchronization, modifying the general structure of the power converter control. Other strategies partially integrated the PLL as an external loop in order to properly emulate inertia as in [16], where the inertial is emulated by the effect of a PLL and the power converter is controlled by an active power controller regulating the electromotive force, highly reducing the possibility of loss of synchronism on the control. Although these strategies were effective in preserving the synchronous behavior in the electrical network, while keeping the current controller in the center, the need to modify the power control structure seems not to be welcome by power conversion manufacturers, which had to change the classical PLL approach with traditional active power regulators to this new one based on power.

In order to avoid firmware changes in all power conversion devices, some works proposed the deployment of a central synchronous emulation structure to manage the inertial support in already installed equipment [17], [18]. Those structures were based on communications links with a centralized control unit responsible of providing synchronous power references to be tracked by the inverters. Even though this idea overcomes some of the challenges regarding the control upgrade in already installed equipment, there are still some functionalities, such as the blackstart or island operation, that cannot be performed based on communications, due to their inherent delay. Lately, new approaches for the synchronous generation have been presented using the VA structure to integrate the synchronous behavior into power converter control. References [19] and [20] presented a generic approach for PLL based grid-forming converter. These strategies rely on the PLL to generate the grid-forming characteristic. However, to emulate inertia it is still necessary to use the swing equation.

This paper presents an IPLL, which simplifies the integration of the swing equation into the PLL voltage synchronization structure by means of reorganizing the internal structure. Furthermore, the VA in the IPLL system is able to generate the necessary transient current reference to maintain the system synchronized with the grid while providing dynamic support, not only for frequency, but also for voltage events. Furthermore, this behavior provides the IPLL with all grid-forming capabilities. Hence it can be used in power converters that requires to operate seamless in on-grid and off-grid conditions. This grid-forming structure can be described as a transitional grid-forming strategy which only provides support during voltage and frequency events at the grid side.

The paper is structured as follows, in section II the conventional PLL structure is presented with the VA approach. In section III the transition from the conventional structure to the IPLL is analyzed and parametrized. In section IV the mathematical model is presented with a pole movement analysis comparing three different systems. Finally, in sections V and VI the system is tested in a HIL real-time simulation as well as in an experimental setup to validate the good performance of the proposed IPLL integrated in a digital signal processor (DSP) based control board.

II. CONVENTIONAL CONTROL AND VIRTUAL ADMITTANCE

The need for integrating grid support functionalities in generation systems controlled though power converters started at the beginning of this century. In fact, over the years the grid codes have become more demanding, setting new operation requirements, especially in the case of grid-connected systems and its transient response in front of grid contingencies [21]. A common feature in almost all inverters installed in the world for grid-tie generation purposes is that they count on a PLL [22]. In current controlled devices, this PLL is in charge of estimating the grid voltage phase and magnitude to ensure a fast synchronization for the internal control of the converter. In renewable energy systems, such as PV systems,
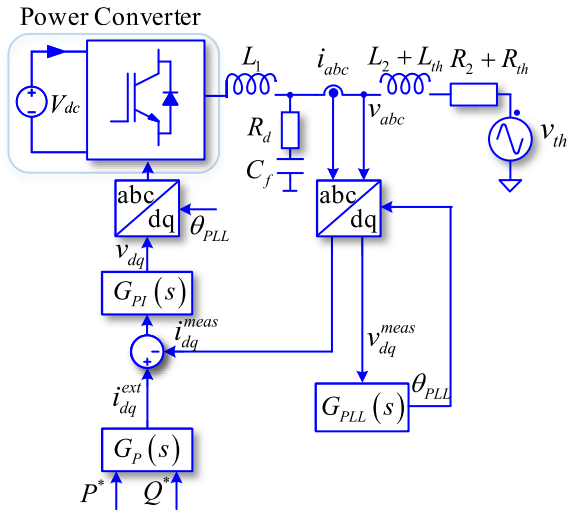
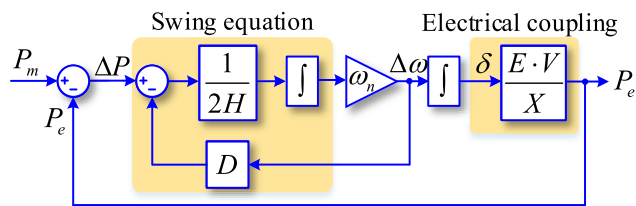**FIGURE 1.** Traditional grid-tied control of a power converter.

FIGURE 2. Generic swing equation implementation on power converters.

FIGURE 3. Virtual admittance structure with traditional PLL structure.
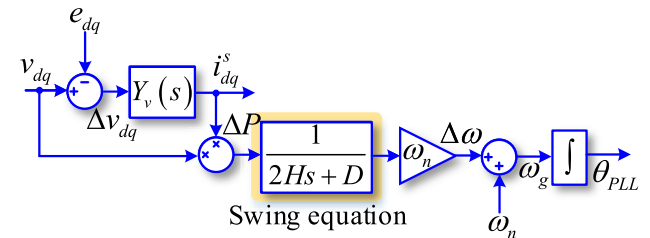
FIGURE 4. Possible swing equation representation.

an inner control loop is responsible of controlling the output current of the power converter based on the estimation performed by the PLL [23], a typical implementation is depicted in Fig. 1. These converters are known as grid-following inverters, and they need to be connected to an external grid in order to be able to control the active and reactive power delivery. Most of the approaches rely on the injection of the maximum power, as in the case of solar or wind power systems, which leads finally to a power control over the dc bus. Even though this control is robust in the case of strong grids, it has a stability issues when connected to grids with a low short-circuit ratio (SCR) [24], [25] or in microgrids applications [26].

The control structure depicted in Fig. 1 provides no support to the grid, it simply behaves as a current source responsive to the active and reactive power references. In the aim of providing new features oriented to improve grid stability many researchers have proposed solutions based on the emulation of synchronous generators. Such generators are the backbone of the electrical energy system [27] and combine the power production with an inherent capacity of stabilizing the grid voltage and frequency in interconnected systems. Therefore, it seems feasible that by using the fast dynamic response of a power converter integrating the swing equation of a synchronous generator, an inverter would be able to easily emulate inertia [28]. This emulation is generally achieved by using the equivalent transfer function of the diagram in Fig. 2,
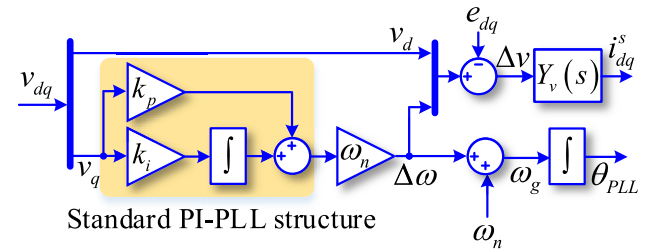
where the parameters of inertia constant and damping allows the system to provide the desired inertia and damping like a synchronous generator.

In [20] the first approach for a PLL based grid forming strategy was presented. In that paper, the PLL was used to synchronize to the electrical grid, as well as to determine the necessary amount of synchronous current to compensate for voltage and frequency variations. Even though the system presented a robust performance, both in grid-tied and isolated applications, the lack of inertial response made the system unable to mitigate the fast RoCoF. The layout of this first approach is shown in Fig. 3, where the components v_{dq} and e_{dq}, represent the grid voltage and the internal electromotive force of the virtual machine. In this approach v_d and $\Delta\omega$ were used to generate the synchronous compensation current for the power converter. In the case of a standard PLL, the component v_q is always zero in steady state, meaning that there is no phase displacement in the phase angle. In order to add a frequency response through the VA, the component accumulating the error in frequency is the variable $\Delta\omega$, which is then used to calculate the frequency error in the compensation system.

III. INERTIAL PHASE-LOCKED LOOP

Considering the structure of Fig. 3 as the basis, the system can be modified to integrate the swing equation transfer function in order to emulate inertia. The resulting layout is shown in Fig. 4.

In this approach the system calculates the difference between v_{dq}, as the point of common coupling (PCC) voltage, and e_{dq}, as the virtual electromotive force of the synchronous generator. Hence, the synchronous current generated through the VA is only active when there is a mismatch between voltage vectors, meaning that this synchronous behavior will
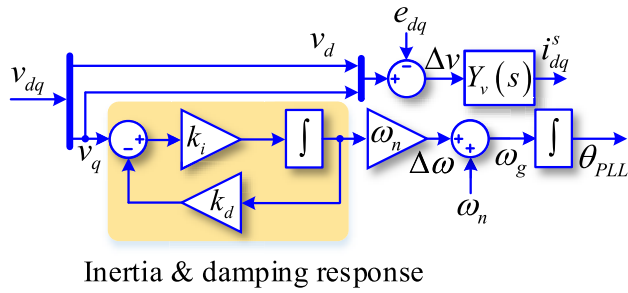
FIGURE 5. IPLL base control schematic.
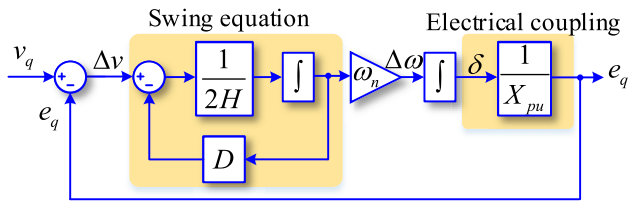
FIGURE 6. IPLL parameters calculation.

only appear during grid disturbances, as v_{dq} will synchronize to e_{dq} in the steady state. In order to be synchronized with the grid, both vectors v_{dq} and e_{dq} must be in phase, which leads to a no current injection through the VA. Due to the use of the synchronization structure, the component e_{dq} can be always determined by an static voltage reference, emulating that the system is always perfectly synchronized to the grid frequency. Even though this proposal is an effective solution to integrate the inertial and damping support of a synchronous machine into the power converter control, it is necessary to make an important change in the synchronization unit, which lead to a higher implementation complexity specially in industrial converters which rely mostly on the PLL and current control structure. To overcome this issue, an IPLL strategy is proposed in this paper, which slightly modifies the classical PLL strategy in order to generate virtual inertial response in an equivalent way of the swing equation, making it suitable for operation in most traditional grid-tied strategies.

The concept of the IPLL strategy is based on the fact that the inertial support is determined by the dynamic response of the internal electromotive force, e_{dq}, during a phase mismatch to the PCC voltage, v_{dq}. Using this delayed response in the synchronization to generate synchronous current, the system is able to emulate the behavior of the swing equation. The schematic in Fig. 5 shows the base control schematic of the IPLL strategy.

As well as in the case of traditional PLLs, the vector v_{dq} is used to synchronize with the grid voltage. However, the standard PI controller is replaced by a low pass filter with specific parameters to emulate the inertial behavior, providing all grid-forming functionalities to the admittance. It is worth to mention that the VA generates the grid-forming support through the dynamic adjustment of the current reference. This new reference allows the system to have a natural and seamless connection with the grid, which enables the converter to perform a blackstart or even work in island mode.

(a)

(b)
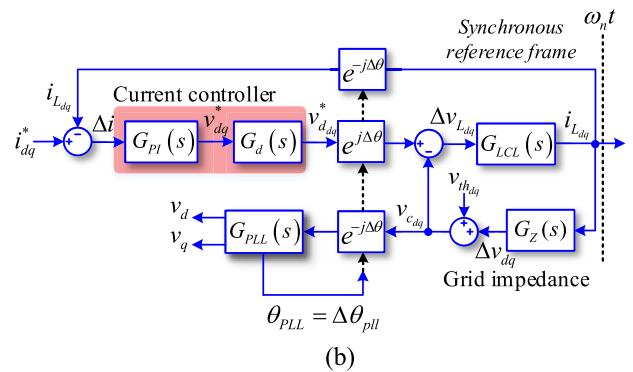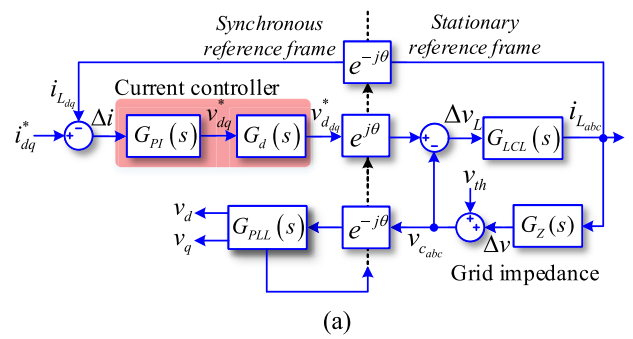
FIGURE 7. Stationary to synchronous reference frame current control using a standard PLL. (a) Synchronous and stationary reference frame coupled diagram (b) Synchronous reference frame used for the analysis.

In order to properly tune the parameters k_i and k_d of the IPLL to emulate inertia and damping, the following per unit transfer function can be obtained from the traditional swing equation transfer function in the power domain, Fig. 2. This function lead to vector v_q to be equivalent to phase angle difference per unit, δ, by means of the VA coefficient, X_{pu}, which is the predominant inductive value on the emulated synchronous machine. This parameter is also in charge of determining the amount of power generated at the output of the converter, as it is defining the output admittance parameter as well. The IPLL parameters k_i and k_d can then be mathematically expressed as (1) and (2), linking the control scheme in Fig. 5 to the equivalent voltage swing equation in Fig. 6.

$$k_i = \frac{1}{2 \cdot H \cdot X_{pu}} \tag{1}$$

$$k_d = D \cdot X_{pu} \tag{2}$$

In these equations the parameters H and D, represent the inertia constant and the damping introduced by the windings of the synchronous generator respectively, and X_{pu} represents the per unit VA parameter. The parameter D can be defined as a function of the power of the VA per unit, the virtual inertia coefficient and the desired damping factor.

$$D = 4 \cdot \xi \cdot \sqrt{\frac{\omega_n \cdot H}{2 \cdot X_{pu}}} \tag{3}$$

IV. MATHEMATICAL ANALYSIS
In this analysis three different models are considered for pole locus comparison: a standard current controller, a current

controller with a conventional PLL and VA, and a current controller with an IPLL and VA. The structure of each model share the same blocks, a current controller, a time delay for the equivalent delay over the sampling time of the PWM signal, the synchronization system, the output LCL filter and the grid determined by its short circuit ratio (SCR). The system has been analyzed in the dq0 synchronous reference frame, to consider the effect of the phase angle rotation introduced by the Park transformation.

A. ABC-STATIONARY TO DQ0-SYNCHRONOUS REFERENCE FRAME

In Fig. 7(a) the schematic shows the existing coupled structure between the control in the synchronous reference frame, and the voltage and currents at the output of the power converter on the stationary reference frame. The PLL is in charge of modifying the phase angle of the system in order to rotate at the same speed as the *abc*-stationary reference frame. In order to rotate everything into the *dq0*-synchronous reference frame, the nominal frequency of the system has to additionally rotate the external components, which leads finally to the schematic of Fig. 7(b). In this figure it can be seen that the nominal frequency that would create θ_{PLL} is extracted from the PLL output and only the component $\Delta\theta_{pll}$ is used. Moreover, the input *dq* components of the voltage in the PLL are forwarded to the output of the transfer function. The transfer function of the output filter and the grid impedance is transformed into the *dq0* frame. This allows a much easier pole analysis as it reduces the complexity of analyzing the system.

B. SYNCHRONOUS MODEL DEFINITION

The relationship between Δv_q and $\Delta\theta$ in a standard PLL approach can be mathematically written as:

$$G_{\Delta\theta}(s) = \frac{k_p^{pll} s + k_i^{pll}}{s^2 + k_p^{pll} s + k_i^{pll}} \quad (4)$$

However, for the IPLL structure the equivalent transfer function between Δv_q and $\Delta\theta$ is modified. In this case the pole on the numerator is nonexistent due to the elimination of the direct k_p^{pll} path. Finally, the resulting equation can be expressed as:

$$G_{\Delta\theta}(s) = \frac{k_i^{pll}}{s^2 + k_d^{pll} \cdot k_i^{pll} \cdot s + k_{pll}} \quad (5)$$

The plant of the system composed of an LCL filter can be described as shown in equation (6).

$$G_{LCL}(s) = \frac{Y_1 \cdot (Z_c Y_2 + 1)}{Z_c (Y_1 + Y_2) + 1} \quad (6)$$

where Y_1, Y_2 and Z_c are the result of shifting the LCL filter from the stationary reference frame to the synchronous
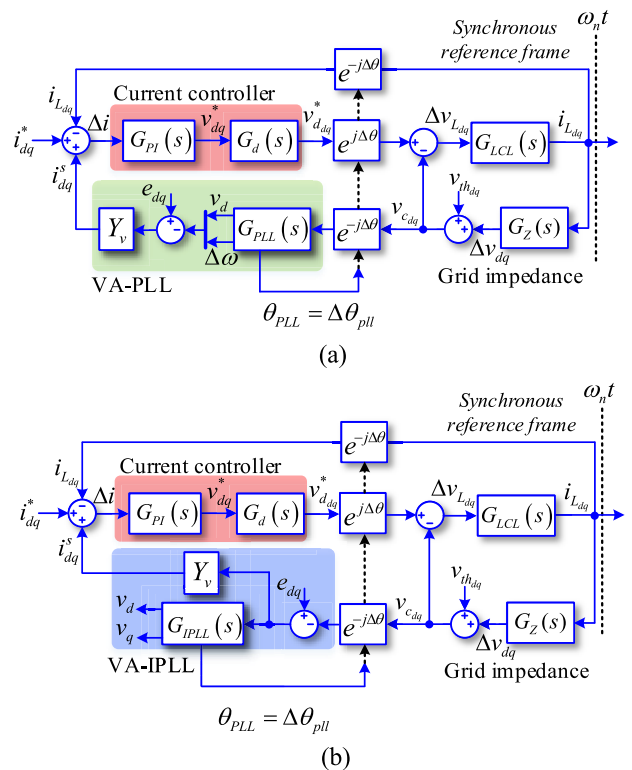

FIGURE 8. Current controllers combined to VA and the synchronization block (a) VA and traditional PLL structure (b) VA and IPLL structure.

reference frame.

$$Y_1(s) = \begin{bmatrix} L_1 s + R_1 & -\omega L_1 \\ \omega L_1 & L_1 s + R_1 \end{bmatrix}$$
$$\times \frac{1}{s^2 L_1^2 + 2L_1 R_1 s + R_1^2 + L_1^2 \cdot \omega^2} \quad (7)$$

$$Y_2(s) = \begin{bmatrix} L_2 s + R_2 & -\omega L_2 \\ \omega L_2 & L_2 s + R_2 \end{bmatrix}$$
$$\times \frac{1}{s^2 L_2^2 + 2L_2 R_2 s + R_2^2 + L_2^2 \cdot \omega^2} \quad (8)$$

$$Z_c(s) = \begin{bmatrix} C_f R_d s^2 + s + C_f R_d \omega^2 & -\omega \\ \omega & C_f R_d s^2 + s + C_f R_d \omega^2 \end{bmatrix}$$
$$\times \frac{1}{C_f (\omega^2 + s^2)} \quad (9)$$

The values of $[L_1, R_1]$ and $[L_2, R_2]$ correspond to the first and second inductance parameters, whereas $[C_f, R_d]$ are the capacitor value and the passive damping resistor of the filter respectively. To include the grid impedance, an additional term can be included in the second inductance transfer function:

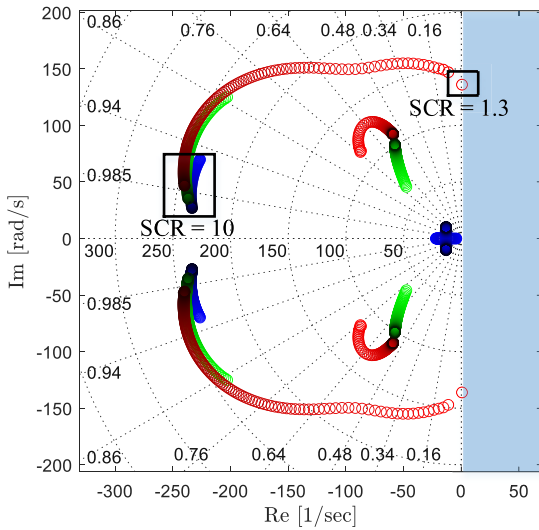$$L_{eq} = L_2 + L_g \quad (10)$$
$$R_{eq} = R_2 + R_g \quad (11)$$

FIGURE 9. SCR shift from 1.3 to 10. (red) Current control with traditional PLL, (green) VA with PLL structure, and (blue) VA with IPLL structure.
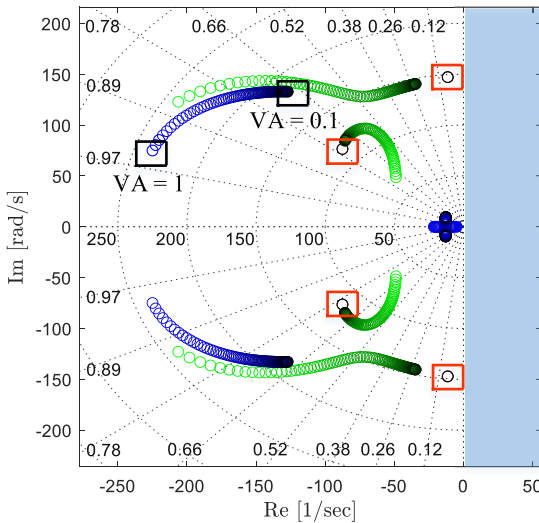

FIGURE 10. Virtual admittance shift from 1 to 0.1 considering a grid SCR = 2. (redsquare) Current control with traditional PLL, (green) VA with PLL structure, and (blue) VA with IPLL structure.

To model the PWM time delay a second order Padé approximation is used to rationalize the delay factor.

$$G_d(s) = \frac{12 - 6T_d s + T_d^2 s^2}{12 + 6T_d s + T_d^2 s^2} \quad (12)$$

Finally, the current controller and the VA can be described as shown in equations (13) and (14) respectively.

$$G_{PI}(s) = \begin{bmatrix} k_i + k_p s & 0 \\ 0 & k_i + k_p s \end{bmatrix} \cdot \frac{1}{s} \quad (13)$$

$$Y_v(s) = \begin{bmatrix} L_v s + R_v & -\omega L_v \\ \omega L_v & L_v s + R_v \end{bmatrix} \cdot$$
$$\times \frac{1}{s^2 L_v^2 + 2L_v R_v s + R_v^2 + L_v^2 \omega^2} \quad (14)$$

The resulting schematics are displayed in Fig. 8(a) and Fig. 8(b), which share the conventional structure presented in Fig. 7(b). The systems are analyzed under different grid scenarios where the VA is used considering both control schematics: VA and PLL & VA and IPLL.

C. POLE LOCUS ANALYSIS

To compare the stability improvement between the PLL and the proposed IPLL, a pole locus analysis of each equivalent model is shown in Fig. 9 and Fig. 10 respectively. It is worth to mention that the VA, Y_v, will only affect the control schematics on Fig. 8(a) and Fig. 8(b). As it is well known the traditional power converter controller based on integrating a current controller with a conventional PLL is prone to be unstable when operating in networks with low SCR. This can be easily seen in Fig. 9 where the PLL with current control structure (red signal) is almost unstable when reaching a SCR close to 1.3. On the other hand, when the VA is added into the PLL model the stability of the system is improved, as shown in Fig. 9 (green signal). This is due to the fact that it provides a wider range of operation to the current control by dynamically adjusting the current reference.

This support provided by the VA not only contributes to the current control stability but it also permits to provide other grid-forming functionalities to the power converter. Furthermore, when considering the IPLL structure for the synchronization unit (blue signal) the power converter enables virtual inertia emulation and power oscillation damping, extending the damping of the poles. It can be clearly seen from Fig. 9 that the combination of the VA and the IPLL contributes to increase the damping of poles, without harming the dynamic operation of the system. This is clearly seen when the SCR is increased to 10, where all systems are moving towards the exact same pole placement.

The effect of the VA can be seen in Fig. 10. In this diagram the evolution of the poles is shown considering, a PLL and VA (green signal), and an IPLL with VA (blue-signal). In both cases the value of the VA changes, showing that the poles move towards the unstable plane when the VA decrease its support. Even though the VA significantly decreases its control action over the current controller, the dynamic support offered by the admittance connection increases the damping of the poles present in the traditional current control with PLL. Furthermore, depending on the amount of VA, the dynamic behavior of the system can be controlled to inject or absorb the desired amount of active and reactive power during transients, giving rise to an adaptable system that enables all grid-forming functionalities when considering the structure that integrates the IPLL with the VA approach. Even with a small value of VA in the system, the poles are still far from the unstable area in the IPLL control strategy, meaning that with a small amount of VA the system will increase its damping capacity. In this regard, to ensure a similar behavior as a synchronous generator the VA has been selected to be 0.3 pu which is equivalent to the subsynchronous impedance of the
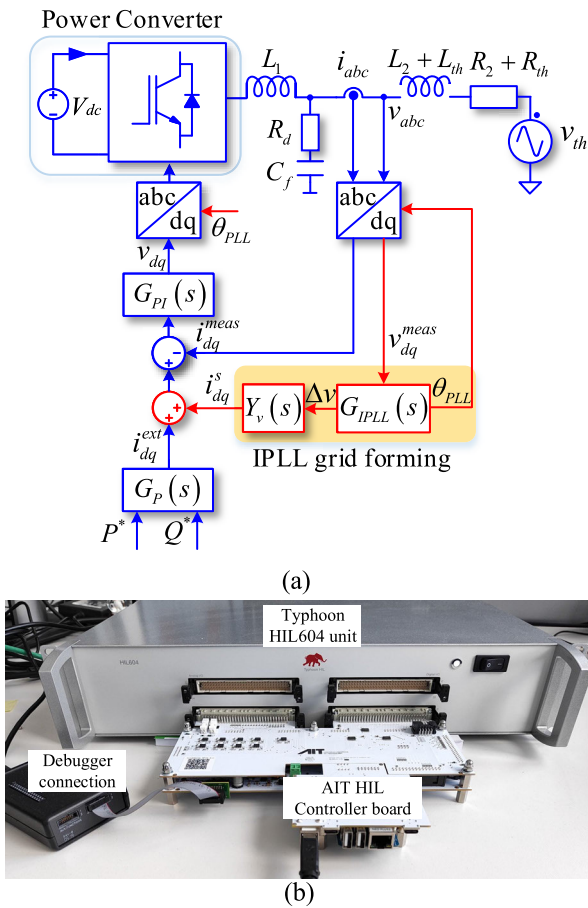
Power Converter

(a)

(b)

FIGURE 11. (a) Electrical schematic of the system including the IPLL structure (b) Real-time simulation hardware setup.

TABLE 1. Real-time simulation and experimental parameters.

Symbol	Definition	Values
Sn	Converter nominal power	35 kVA
SCR	Short circuit ratio	1
L1	Inverter-side inductance	460 µH
Cf	Capacitance	13.6 µF
Rd	Damping resistance	0.5 Ω
L2	Grid-side inductor	55 µH
Rv	Initial virtual resistor	0.46 Ω
Lv	Initial virtual inductor	0.00442 H
ωn	Nominal frequency	314.15 rad/s
k_d^{pll}	Initial PLL kp	11.56
k_i^{pll}	Initial PLL ki	0.33
kp_cc	Current control kp	4.5
ki_cc	Current control ki	1000
Hv	Virtual inertia	5
ξv	Virtual damping	1
Hg	Synchronous generator Inertia	5
ξg	Synchronous generator Damping	0.3

generator and the resistance has been intentionally increased to 0.1 pu to obtain an increased damping factor in the VA.
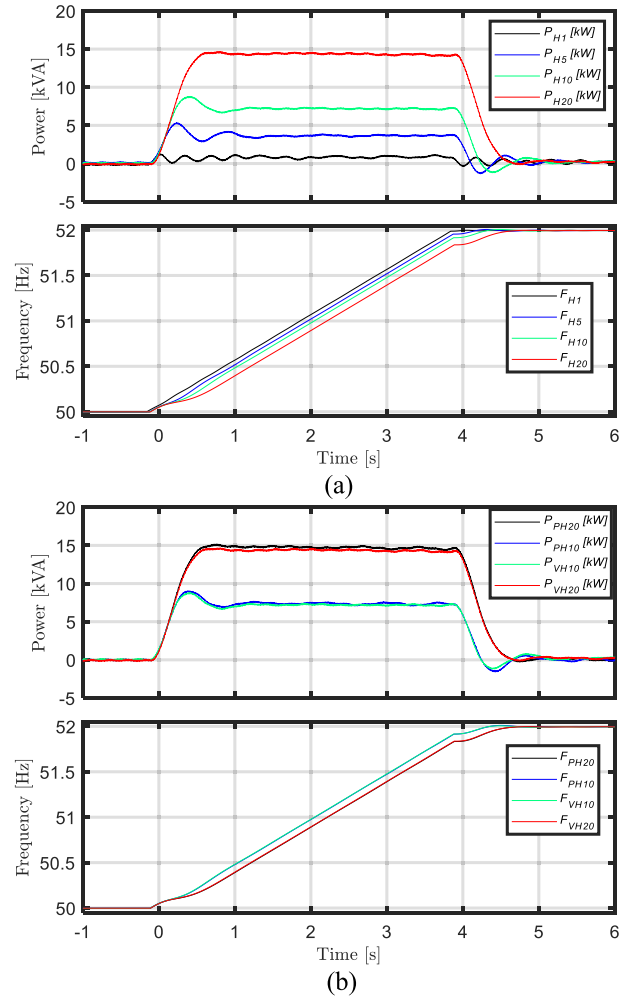

(a)

(b)

FIGURE 12. Inertia emulation with the IPLL structure (a) IPLL under different inertia coefficients, (b) comparison between IPLL and traditional swing equation.

V. REAL-TIME SIMULATION RESULTS

The electrical schematic for both the real-time simulation and the experimental setup is presented in Fig. 11. The system is composed of a four-wire three-level T-type power converter topology connected to a synchronous generator with specific parameters of inertia and damping, Table 1. The real-time simulation setup is composed of a Typhoon HIL 604 unit, to emulate the physical elements of the electrical network, considering the inertial grid, a 20 kW load, and the power converter. Furthermore, above proposed control structures are implemented on an AIT HIL controller to control the power converter under different grid scenarios.

A. INERTIA EMULATION: FREQUENCY EXCURSION

In this first case, the inertia emulation is tested, giving rise to the results shown in Fig. 12. In this scenario a constant RoCoF, that follows a slope of 0.5 Hz/s during 4 seconds in the grid is considered. The power converter emulating inertial response reacts by injecting a constant power to support the frequency contingency. This power capacity will be higher if
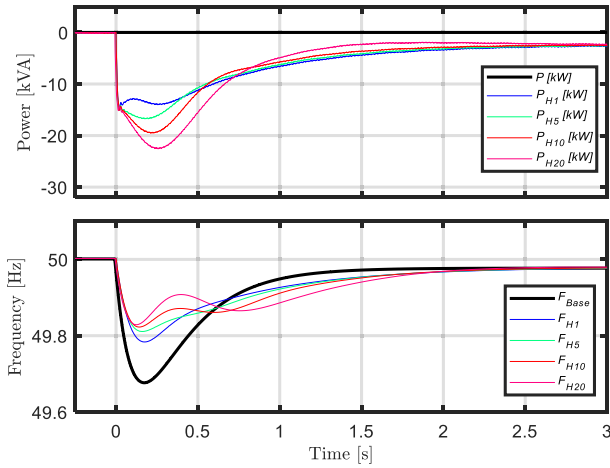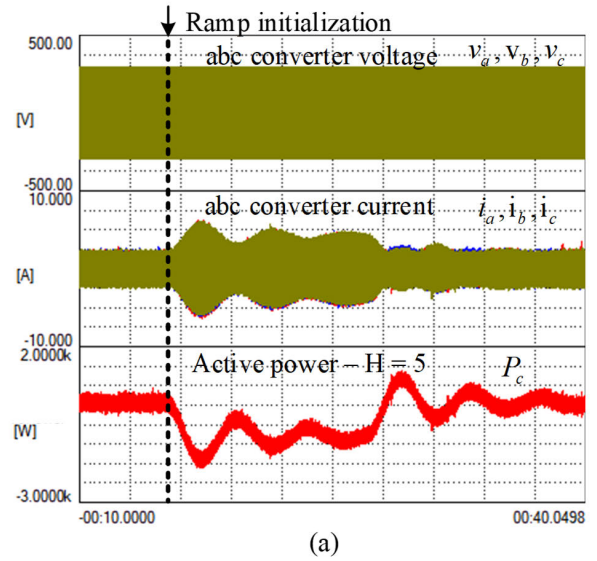
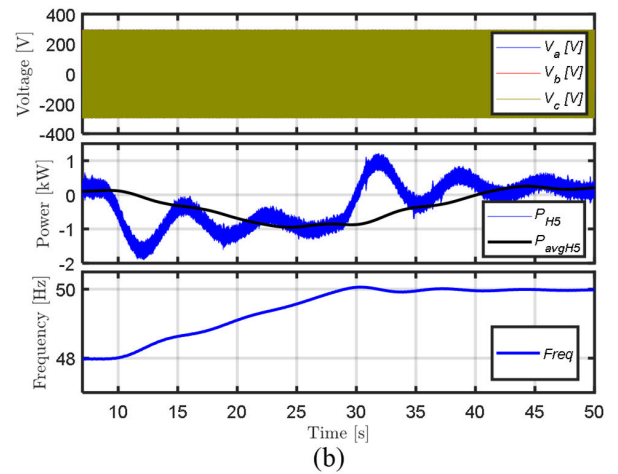**FIGURE 13.** 20kW load connection to the grid and support from the power converter using the IPLL structure.

FIGURE 14. Experimental setup (a) back-to-back setup of the AIT-SGC converters, (b) synchronous generator setup.

the inertia constant, H, increases, as it is shown in the upper graphic, Fig. 12(a). In fact, to calculate the inertial power for a given constant of inertia at the power converter the following mathematical equation can be used [27]:

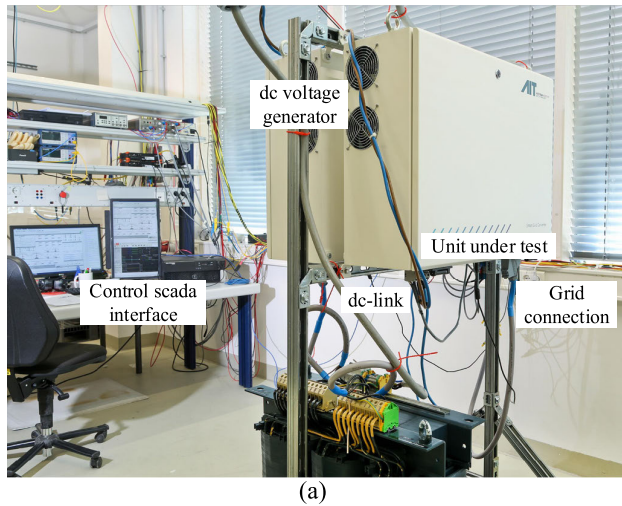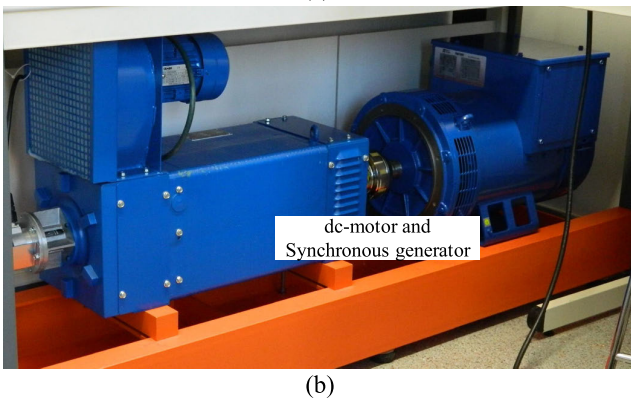$$P_H = \frac{2 \cdot \pi \cdot \text{RoCoF} \cdot 2 \cdot H \cdot S_n}{\omega_n} \quad (15)$$

FIGURE 15. Inertial support during constant RoCoF of 0.1 Hz/s, (a) experimental result (b) frequency excursion during the inertial support.

This equation determines that for $H = 1$, the active power provided by the power converter is below 1 kW. When the constant of inertia is increased above the initial value to 5, 10 and 20, the respective active power support is incremented to 3.5 kW, 7 kW and 14 kW respectively. This can be observed in Fig. 12(a), which shows that the power delivered to the grid matches the one calculated for the specific RoCoF and inertia constant. In order to ensure that the inertia emulation displayed in Fig. 12(a) is having the same dynamic response as the traditional swing equation implementation on transient domain, both systems are compared in Fig. 12(b) for inertia constants 10 and 20, where the IPLL structure and the swing equation structure are represented by subindex VH and PH respectively in the legend, giving rise to the same dynamic response under the RoCoF.

B. INERTIA EMULATION: LOAD CHANGE

In the second case, the load at the PCC is suddenly connected giving rise to a frequency drop in the synchronous generator,
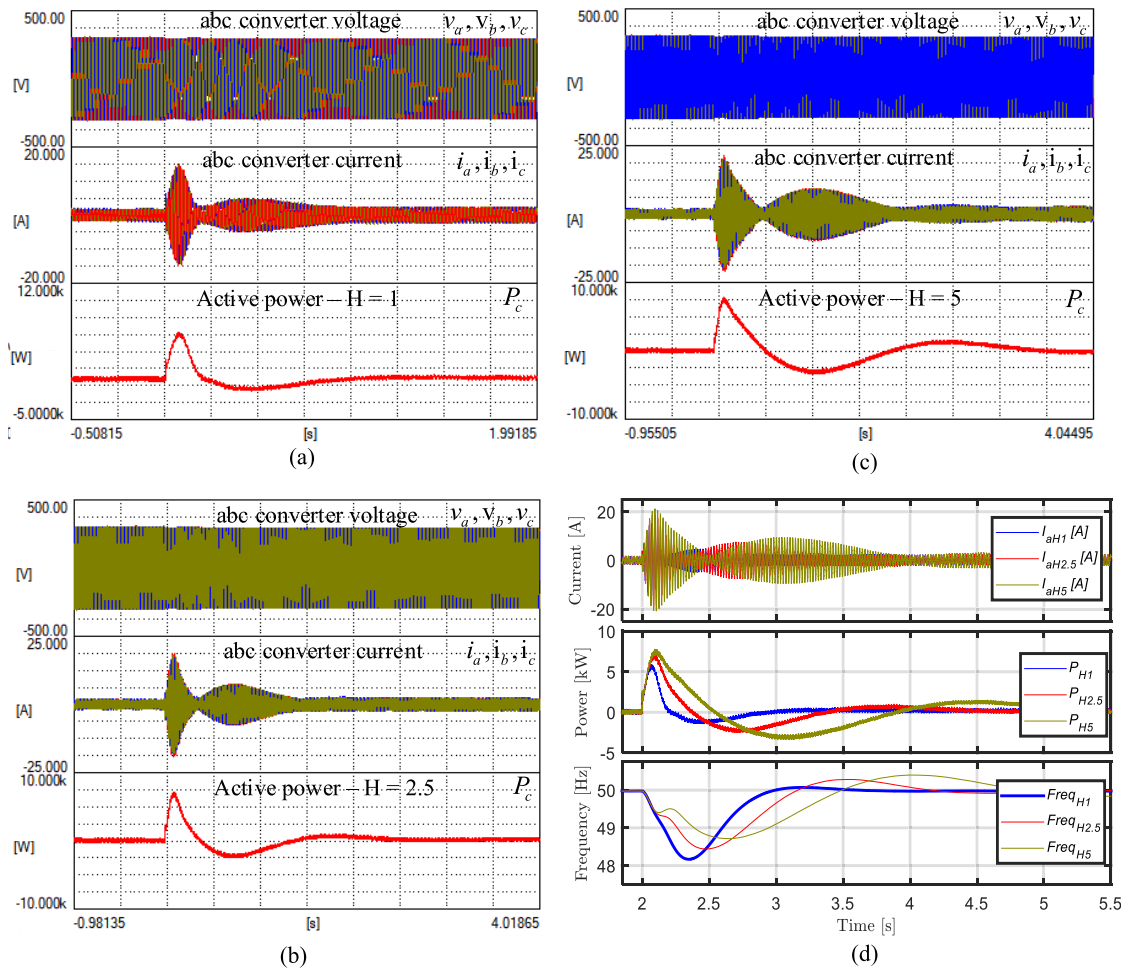
FIGURE 16. 20kW load connection with different inertial coefficients. (a) inertia constant set to 1, (b) inertia constant set to 2.5 (c) inertia constant set to 5, and (d) comparison between the different inertial coefficient.

as shown in Fig. 13. During the event the converter will provide dynamic support to reduce the frequency drop in the system. It can be observed in Fig. 13 that, due to the low inertia and damping of the grid, the system frequency drops to a minimum value of 49.7 Hz, and takes around one second to recover close to the nominal frequency in the base case. Once the power converter is enabled with the IPLL structure, it provides dynamic support to the grid during the load transient. The initial power contribution to the frequency contingency on the power converter is provided by the VA, which detects an instantaneous difference between vectors, v_{dq} and e_{dq}, representing the grid voltage and the virtual electromotive force. After this initial contribution from to the VA, the inertial response of the IPLL generates the necessary current reference to provide the dynamic support to the grid during the frequency contingency. The higher the inertial constant set on the power converter the higher the support provided during the event. Comparing the different transient curves, it is possible to see a reduction from 49.7 Hz in the base case to a value of 49.85 Hz in the case with higher inertial constant.

VI. EXPERIMENTAL RESULTS

The experimental setup used for the experimental results is presented in Fig. 14. The picture in Fig. 14(a) shows the back-to-back setup of two AIT smart grid converters (SGC) of 35 kVA rated power, 4-wires 3-level T-type converter topology. One of the units is used as a dc-voltage generator to create a stable dc-link voltage to the unit under test. The other unit is integrated with the IPLL strategy for the experimental results. In addition to the converter setup the picture in Fig. 14(b) shows the synchronous generator setup, which has a rated power of 30 kVA.

The experimental results are separated into two study cases. The first one is related to the inertia emulation under a certain RoCoF of the synchronous generator. In this case, the synchronous generator will have a specific rate of change at the output frequency, which the converter under test will detect and inject the necessary amount of active power to counteract the contingency. After the event the system will return to the operation point prior to the frequency shift. The second test highlights the inertial response of the converter under a load change at the PCC, showing specifically the

dynamic response of the converter with different inertia constants. In order to create the frequency perturbation, a 20 kW load is connected at the synchronous generator output.

A. INERTIA EMULATION: FREQUENCY EXCURSION

The equation to determine the inertia power support under a constant RoCoF of the grid voltage has been presented in (15), which relates the rate of change to the amount of inertia constant depending on the nominal power of the converter. In this case scenario, the inertia constant has been set to H = 5 and the damping coefficient k_d^{pll} has been set to a value of 0. This elimination of the damping component makes the system prone to oscillations if the synchronous generator has not sufficient damping coefficient. The synchronous generator parameters for the inertia and damping are shown in Table 1. During the frequency event the power converter will inject a constant power depending on the RoCoF. It is possible to see in Fig. 15(b) that the frequency moves initially from a value of 48 Hz to 50 Hz in 20 s, which leads to a rate of change of 0.1 Hz/s. Using the equation presented above, (15), the equivalent inertial power should be 0.7 kW. Fig. 15(a) show that the power is underdamped due to the elimination of the damping factor in the IPLL structure, thus all the damping effect is provided by purely from the synchronous generator, giving rise to small power oscillations.

B. INERTIA EMULATION: LOAD CHANGE

In the second case, a load of 20 kW is connected to the PCC, which will force the synchronous generator to feed the load, thus reducing the grid frequency depending on the inertia and damping factor of the device. Three different cases have been tested under the experimental setup, where in each case the damping factor of the IPLL structure has been eliminated to highlight the effect of the inertial response during the event. The inertia constant has been modified from an initial value of 1 to two different values, 2,5 and 5 respectively.

It is possible to observe from Fig. 16, when the IPLL structure detects a mismatch between the PCC voltage, v_{dq}, and the internal electromotive force, e_{dq}, which leads to an instantaneous current injection. After the initial power injection of the VA, the grid frequency gets back to its nominal value. This is detected by the IPLL that adjusts the amount of inertial response to correct the frequency displacement. Fig. 16(d) shows a comparison of the results obtained with different inertia constants used in the experiment. It should be noted that the initial power step is similar in the three cases as it purely depends on the VA value which provides this first current reaction.

VII. CONCLUSION

This paper has presented the mathematical structure, and the real-time and experimental results of the IPLL control structure for a power converter control. This structure presents huge benefits in terms of implementation and integration within a standard deployed unit, which is granted with all grid-forming capabilities with just a minor change in the

synchronization structure. This paper has focused specifically on the inertia emulation capacity and the high improvement on the pole placements when utilizing the IPLL strategy. The mathematical analysis has shown high benefits in the use of the VA to generate synchronous current compensation in the system, which are even greater when interconnected with the inertial support provided by the IPLL. The easy implementation of the proposed control, in terms of modification of the power control structure in the power converter, enables a simpler path for emulating a natural support of the inertia component and provides grid-forming functionalities to the power converter. Moreover, this enhanced loop allows the system to impose to the power converter a more natural exchange of power during grid contingencies. Depending on the value of the VA the amount of support can be dynamically modified to shift the behavior of the converter to a more damped operation. This flexibility on the tuning allows the converter to emulate different inertia constant and current injection during transients.

HIL and experimental results have been presented to display the benefits of the IPLL control structure. The system has been tested under a specific RoCoF where the power converter provides the desired inertial response depending on the inertial constant and VA set on the system. The dynamic response of the IPLL system has been compared to the response of the traditional swing equation, giving rise to the same performance with a simpler structure. The inertial support has also been tested under a load connection on a synchronous generator with low damping capacity, leading to a reduction of the RoCoF as well as the minimum frequency drop at the system.

The easy implementation of the control structure makes this solution a cost-effective approach for newly integrated grid-forming power converter connected to grid. By means of tuning the IPLL with the desired inertia and damping the system will respond as a classical synchronous generator with grid-forming functionalities during faults, while operating as a grid-following unit in grid-tied applications. This takes the most of both control modes with the same controller, with no need to changing the controller structure or tapping between control modes. Further research on the IPLL will be carried out with different standard active power controllers on renewable energy systems to highlight the benefits of the structure.

REFERENCES

[1] *ENTSO-E Position Paper Stability Management in Power Electronics Dominated Systems? A Prerequisite to the Success of the Energy Transition ENTSO-E Mission Statement*, Eur. Netw. Transmiss. Syst. Oper. Electr. (ENTSO-E), 2022.

[2] *Frequency Stability Evaluation Criteria for the Synchronous Zone of Continental Europe*, REE, Terna, TransnetBW, Stuttgart, Germany, 2016.

[3] "SolarPower Europe, Europe EU market outlook," Sol. Power Eur., Annu. Rep., 2021.

[4] F. Blaabjerg, Z. Chen, and S. B. Kjaer, "Power electronics as efficient interface in dispersed power generation systems," *IEEE Trans. Power Electron.*, vol. 19, no. 5, pp. 1184–1194, Sep. 2004, doi: 10.1109/TPEL.2004.833453.

[5] *Need for Synthetic Inertia (SI) for Frequency Regulation—ENTSO-E Guidance Document for National Implementation for Network Codes on Grid Connection*, ENTSO-E, Brussels, Belgium, Mar. 2017.

[6] *Frequency Stability in Long-Term Scenarios and Relevant Requirements*, Project Inertia Team, San Diego, CA, USA, 2021.

[7] J. Fang, H. Li, Y. Tang, and F. Blaabjerg, "On the inertia of future more-electronics power systems," *IEEE J. Emerg. Sel. Topics Power Electron.*, vol. 7, no. 4, pp. 2130–2146, Dec. 2019, doi: 10.1109/JESTPE.2018.2877766.

[8] J. Rocabert, A. Luna, F. Blaabjerg, and P. Rodríguez, "Control of power converters in AC microgrids," *IEEE Trans. Power Electron.*, vol. 27, no. 11, pp. 4734–4749, Nov. 2012, doi: 10.1109/TPEL.2012.2199334.

[9] Q.-C. Zhong and G. Weiss, "Synchronverters: Inverters that mimic synchronous generators," *IEEE Trans. Ind. Electron.*, vol. 58, no. 4, pp. 1259–1267, Apr. 2011, doi: 10.1109/TIE.2010.2048839.

[10] Q.-C. Zhong, P.-L. Nguyen, Z. Ma, and W. Sheng, "Self-synchronized synchronverters: Inverters without a dedicated synchronization unit," *IEEE Trans. Power Electron.*, vol. 29, no. 2, pp. 617–630, Feb. 2014, doi: 10.1109/TPEL.2013.2258684.

[11] J. Roldán-Pérez, A. Rodríguez-Cabero, and M. Prodanovic, "Harmonic virtual impedance design for parallel-connected grid-tied synchronverters," *IEEE J. Emerg. Sel. Topics Power Electron.*, vol. 7, no. 1, pp. 493–503, Mar. 2019, doi: 10.1109/JESTPE.2018.2828338.

[12] M. P. Kazmierkowski and L. Malesani, "Current control techniques for three-phase voltage-source PWM converters: A survey," *IEEE Trans. Ind. Electron.*, vol. 45, no. 5, pp. 691–703, 1998, doi: 10.1109/41.720325.

[13] A. Gonzalez-Cajigas, J. Roldan-Perez, and E. J. Bueno, "Design and analysis of parallel-connected grid-forming virtual synchronous machines for island and grid-connected applications," *IEEE Trans. Power Electron.*, vol. 37, no. 5, pp. 5107–5121, May 2022, doi: 10.1109/TPEL.2021.3127463.

[14] P. Rodríguez, C. Citro, J. I. Candela, J. Rocabert, and A. Luna, "Flexible grid connection and islanding of SPC-based PV power converters," *IEEE Trans. Ind. Appl.*, vol. 54, no. 3, pp. 2690–2702, May 2018, doi: 10.1109/TIA.2018.2800683.

[15] A. Tarraso, N.-B. Lai, G. N. Baltas, and P. Rodriguez, "Power quality services provided by virtually synchronous FACTS," *Energies*, vol. 12, no. 17, p. 3292, Aug. 2019, doi: 10.3390/en12173292.

[16] P. Imgart, A. Narula, M. Bongiorno, M. Beza, and J. R. Svensson, "A cascaded power controller for robust frequency ride-through of grid-forming converters," in *Proc. IEEE Energy Convers. Congr. Expo (ECCE)*, Mar. 2022, pp. 1–8, doi: 10.1109/ECCE50734.2022.9947721.

[17] C. Verdugo, A. Tarraso, J. I. Candela, J. Rocabert, and P. Rodriguez, "Centralized synchronous controller based on load angle regulation for photovoltaic power plants," *IEEE J. Emerg. Sel. Topics Power Electron.*, vol. 9, no. 1, pp. 485–496, Feb. 2021, doi: 10.1109/JESTPE.2020.2995339.

[18] N.-B. Lai, A. Tarrasó, G. N. Baltas, L. V. M. Arevalo, and P. Rodriguez, "External inertia emulation controller for grid-following power converter," *IEEE Trans. Ind. Appl.*, vol. 57, no. 6, pp. 6568–6576, Nov. 2021, doi: 10.1109/TIA.2021.3108350.

[19] L. Harnefors, M. Schweizer, J. Kukkola, M. Routimo, M. Hinkkanen, and X. Wang, "Generic PLL-based grid-forming control," *IEEE Trans. Power Electron.*, vol. 37, no. 2, pp. 1201–1204, Feb. 2022, doi: 10.1109/TPEL.2021.3106045.

[20] A. Tarrasó, J. I. Candela, N. B. Lai, G. N. Baltas, and P. Rodriguez, "Virtual admittance PLL structure for grid-forming power converters in microgrids," in *Proc. IEEE Energy Convers. Congr. Expo. (ECCE)*, Jan. 2020, pp. 5007–5011, doi: 10.1109/ECCE44975.2020.9235629.

[21] N. Grid. (2017). *The Grid Code—U.K.* [Online]. Available: https://www.nationalgrid.com/sites/default/files/documents/8589935310-CompleteGridCode.pdf

[22] P. Rodriguez, J. Pou, J. Bergas, J. I. Candela, R. P. Burgos, and D. Boroyevich, "Decoupled double synchronous reference frame PLL for power converters control," *IEEE Trans. Power Electron.*, vol. 22, no. 2, pp. 584–592, Mar. 2007, doi: 10.1109/TPEL.2006.890000.

[23] E. Villanueva, P. Correa, J. Rodriguez, and M. Pacas, "Control of a single-phase cascaded H-bridge multilevel inverter for grid-connected photovoltaic systems," *IEEE Trans. Ind. Electron.*, vol. 56, no. 11, pp. 4399–4406, Nov. 2009, doi: 10.1109/TIE.2009.2029579.

[24] Z. Xie, Y. Chen, W. Wu, Y. Xu, H. Wang, J. Guo, and A. Luo, "Modeling and control parameters design for grid-connected inverter system considering the effect of PLL and grid impedance," *IEEE Access*, vol. 8, pp. 40474–40484, 2020, doi: 10.1109/ACCESS.2019.2950933.

[25] S. Maganti and N. P. Padhy, "Analysis and design of PLL less current control for weak grid-tied LCL-type voltage source converter," *IEEE J. Emerg. Sel. Topics Power Electron.*, vol. 10, no. 4, pp. 4026–4040, Aug. 2022, doi: 10.1109/JESTPE.2021.3129804.

[26] W. Wu, Y. Liu, Y. He, H. S.-H. Chung, M. Liserre, and F. Blaabjerg, "Damping methods for resonances caused by LCL-filter-based current-controlled grid-tied power inverters: An overview," *IEEE Trans. Ind. Electron.*, vol. 64, no. 9, pp. 7402–7413, Sep. 2017, doi: 10.1109/TIE.2017.2714143.

[27] N. J. Kundur and P. Balu, *Power System Stability and Control*. New York, NY, USA: McGraw-Hill, 1994.

[28] W. Zhang, A. Tarraso, J. Rocabert, A. Luna, J. I. Candela, and P. Rodriguez, "Frequency support properties of the synchronous power control for grid-connected converters," *IEEE Trans. Ind. Appl.*, vol. 55, no. 5, pp. 5178–5189, Sep. 2019, doi: 10.1109/TIA.2019.2928517.

ANDRES TARRASÓ (Member, IEEE) received the M.Sc. and Ph.D. degrees in electrical engineering from the Technical University of Catalonia, Barcelona, Spain, in 2017 and 2022, respectively. Since 2017, he has been a Research Assistant with the Department of Electrical Engineering and an Assistant Professor of electrical systems subjects. In 2019, he was a full-time Engineer with NRGLab, with a focus on the development of real-time simulation systems interconnected with external devices, to ensure its stability and reliability. Furthermore, he was the leading programmer for several real-time simulation demonstrators in two different industrial projects and has participated in real-time simulation courses as the leading Trainer with Typhoon HIL, integrating HIL devices with custom applications. He is currently with the Polytechnic University of Catalonia (UPC) in the department of electrical engineering within the group Renewable Electrical Energy Systems (SEER), and also an Associated with the Austrian Institute of Technology GmbH (AIT). He is the author of 11 journal articles and 22 papers at international conferences. His current research interests include power electronics, energy storage systems, photovoltaics, wind energy systems, real-time simulation, and microgrids.

JOSE IGNACIO CANDELA (Member, IEEE) received the Ph.D. degree in electrical engineering from the Technical University of Catalunya (UPC), Barcelona, Spain, in 2009. He became an Associate Professor, in 1993, where he later advanced to Full Professor, in 2011. Currently, he is part of the research group on Renewable Electrical Energy Systems, UPC. He has authored or coauthored more than 50 published technical articles and holds several patents. His current research interests include power conditioning, integration of distributed energy systems, and the control of grid-connected power converters. He has been a member of several IEEE societies for more than 20 years.

JOAN ROCABERT (Member, IEEE) received the M.Sc. and Ph.D. degrees in electrical engineering from the Technical University of Catalonia (UPC), Barcelona, Spain, in 2003 and 2010, respectively. From 2004 to 2008, he was a Research Assistant with the Department of Electronic Engineering, UPC. He has been a Researcher and an Assistant Professor with the Department of Electrical Engineering, UPC, since 2008. His current research interests include power electronics, photovoltaics (PVs), wind energy systems, and microgrids.

ZORAN MILETIC (Senior Member, IEEE) received the M.Sc. degree in electrical engineering from the Faculty of Electrical Engineering, University of Belgrade, Serbia, in 1996. He is currently pursuing the Ph.D. degree with the University of Innsbruck, with a focus on multi-level multi-cell power converters for LV power quality applications.

For over two decades, he has been leading the product development of power electronics converters for renewable energy applications with Xantrex Technology Inc., Vancouver, Canada, and Schneider Electric Solar, in both Europe and Canada. Since 2014, he has been a Senior Research Engineer with AIT Austrian Institute of Technology GmbH. His experience includes the design of power electronics and control for solar MPPT charge controllers and single and 3-phase solar inverters from a few KW to several hundreds of KVA. He is the holder of several U.S. and international utility patents. His research interests include grid-connected and grid-forming converters and their control for emerging smart grid applications. He received the Professional Certificate in Power Electronics from the Department of Electrical and Computer Engineering, University of Colorado at Boulder, USA, in 2008.

ALVARO LUNA (Member, IEEE) received the B.Sc., M.Sc., and Ph.D. degrees in electrical engineering from the Technical University of Catalonia (UPC), Barcelona, Spain, in 2001, 2005, and 2009, respectively. He was a Faculty Member with UPC, in 2005, where he is currently an Assistant Professor. His research interests include wind turbine control, photovoltaic systems, integration of distributed generation, and power conditioning.

● ● ●